Scale-free fuse network and its robustness

Carlos Felipe Saraiva Pinheiro* and Americo T. Bernardes†
Departamento de Fisica and REDEMAT, Universidade Federal de Ouro Preto, 35400-000 Ouro Preto, Minas Gerais, Brazil
(Received 26 July 2005; published 20 October 2005)

The robustness and reliability of scale-free networks are tested as a fuse network. The idea is to examine the robustness of a scale-free network when links are irreversibly removed after failing. Due to inherent characteristics of the fuse network model, the sequence of links removal is deterministic and conditioned to fuse tolerance and connectivity of its ends. It is a different situation from classical robustness analysis of complex networks, when they are usually tested under random fails and deliberate attacks of nodes. The use of this system to study the fracture of elastic material brought some interesting results.

DOI: 10.1103/PhysRevE.72.046709 PACS number(s): 05.10.−a, 89.75.−k, 02.70.−c

I. INTRODUCTION

Material science and engineering have always been concerned with robustness and durability of materials where a trade off involving energy consumption, costs, and mechanical reliability is to be optimized. The damage and fracture of materials always involve economic and human costs. Cracking of glass, corrosion of metallic structures and tools, the aging of concrete, and the failure of fiber networks are just a few of many everyday stressing situations leading to material failure.

Different classes of materials have different mechanical and thermal properties. Ceramics are incredibly rigid and thermally resistant, but their failure is catastrophic for their lack of plasticity. Metals are much softer than ceramics, but have thermal restrictions and are way too heavy for certain uses. Weight is not usually a problem with polymers, but excessive creep under heat and degradation under ultraviolet radiation often limit their usage. In that scenario, composites may arise as a solution, combining the best of two materials. The idea is not new. Wood itself is a fibrous composite: cellulose fibers in a lignin matrix. The cellulose fibers have high tensile strength but are very flexible (i.e., low stiffness), while the lignin join the fibers and furnishes the stiffness. Rocks, concrete, Portland cement are all successful examples of composite materials [1].

So it seems to be a fact that inhomogeneity in materials is in many cases desirable. That leads to the problems concerning structures characterized by the lack of conventional geometrical order. Actually, several statistical models for the fracture of disordered media have been proposed and explored in the last few decades (see [2] for a good review). One of them is the random fuse network [3–8], described below, that makes use of the similarity between Hook's law and Ohm's law, trying to apprehend the role of heterogeneity at a mesoscopic level taking to macroscopic failure in elastic materials. The network itself is regular, usually square, the disorder is introduced via dilution (a certain fraction of the fuses is removed) and/or attributing different characteristics to each fuse. In the present work, the disorder is introduced by using a irregular geometry for the network. Not a random network, but a scale free network (SFN).

SFN's have been found to lie behind the structure of many natural and artificially created networks [9]: www [10,11], internet routers [12], proteins [13], and scientific collaborations [14], just to name a few. The main features that distinguish these complex networks from "ordinary" ones are their small-world character [15] and the scale-free degree distribution [16].

The original model to create SFN's was proposed by Albert and Barabasi [17] and was based on growth and preferential attachment. At each time step a new node is added to the network and attaches itself to m already existing nodes with probability proportional to their incidence degrees. With this simple recipe, a scale-free network with degree distribution of exponent 3 is obtained. Some changes and new models have also been proposed, allowing a control of the characteristic exponent and catching different dynamics for growth and even competition between the nodes of the network [18].

Given the abundant examples of complex networks in nature, the problem of attacks on complex networks has attracted a lot of attention recently [19–22]. It has been observed that scale-free networks display an exceptional robustness against random node failure, but show poor performance against preferential node removal (the most connected nodes are preferentially removed).

The robustness of SFN's has also been evaluated using the fiber bundle model [2] as a scenario [23,24]. The nodes were fibers that broke when the load imposed was greater than their individual threshold. But, again, the nodes (fibers) were the entities to be removed. As in the case of the reliability evaluation of power transmission systems [25–27], the present work strives to evaluate the robustness of networks when the *links*, and not the nodes, are subjected to overload. Power systems, however, are not scale-free networks. And, as far as the authors know, this is the first time scale-free networks have their robustness tested under deterministic link failure. If the system is also thought to mimic a fiber reinforced material, it makes a lot more sense thinking of fibers as links instead of nodes, for it is hard to imagine that a single fiber could locally share its load with as many fibers as a hub in a SFN.

*Electronic address: felipe@iceb.ufop.br
†Electronic address: atb@iceb.ufop.br

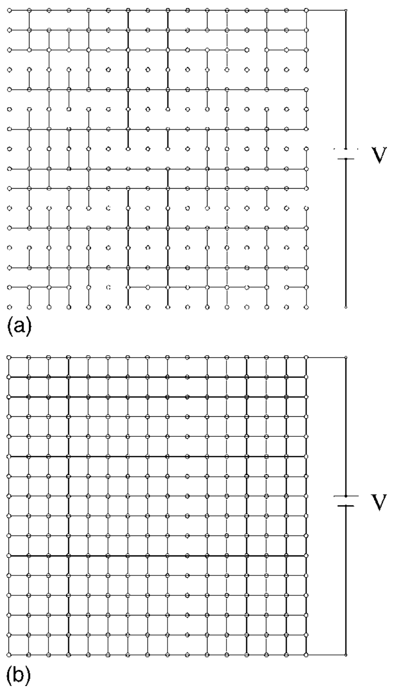

FIG. 1. Two-dimensional square fuse network. (a) Diluted. (b) Regular network.

II. MODEL

In the classical random fuse network model, fuses are placed at random on the bonds of a d-dimensional hypercubic lattice. Figure 1 shows the two-dimensional case. Two busbars are placed across the top and the bottom rows of the network and a voltage difference V is applied between the two bars. The external voltage made sufficiently large will burn a fuse or a few of them and eventually take the system to a complete rupture or breakdown, when no current flows.

The fuses may be identical, i.e. have identical conductivity g_j and identical tolerance i_{cj}, in which case the disorder is introduced by diluting the links in the network, respecting the percolation limit, as in Fig. 1(a).

A different array may be set with a regular square network, as in Fig. 1(b). In that case, disorder comes with a statistical distribution of fuse characteristics (conductivity and/or tolerance).

In the present work, the disorder element is simply the network topology, for SFN's are marked by a power-law degree distribution and short characteristic length [9,28,29]. The possibilities concerning the connectivities of both terminals of each fuse are unlimited (actually it is limited by the maximum connectivity, which, by its turn, is only limited by the size of the network).

The fuse network in square lattices clearly establishes two sets of nodes that are connected to the source terminals via two bus bars, usually the top and the bottom rows of nodes. For a complex network, however, this matter is not clear. What is proposed here is starting from an intuitive notion of peripheral and central regions in the network; we will study three different cases of loading.

The peripheral region is now declared to be the set of all nodes with connectivity $k=m$. These are the nodes that were never connected after being added to the network. They correspond to the nodes with the lowest connectivity in the network and, most likely, the last nodes added to it.

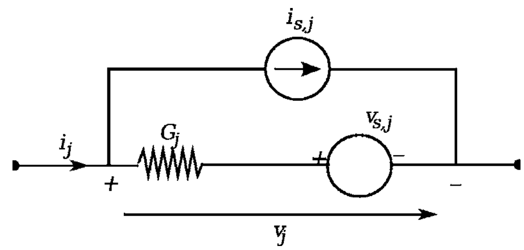

FIG. 2. A typical resistive network element. If it is a voltage source, $i_{s,j}$ is zero; if it is a current source, $v_{s,j}$ is zero; if it is a fuse both $i_{s,j}$ and $v_{s,j}$ are zero.

On the opposite hand, the the central node is defined as the most connected one.

Based on these definitions, three different loading cases are studied:

(1) One terminal of the voltage source is connected to the central node and the other terminal, to the peripheral nodes.

(2) The peripheral region is divided into two sets with the same number of nodes (or differing by one) and each set is connected to a terminal of the voltage source.

(3) A few randomly chosen nonperipheral nodes are connected to one terminal of the voltage source and the peripheral region is connected to the other terminal.

The peripheral nodes are actually merged into a single node, in cases (1) and (3), or two nodes, in case (2). These are sometimes referred as the periphery terminal or the periphery along the text.

III. METHODS

To deal with the terrifying problem of analyzing the complex circuit created by a scale-free network it was made broad use of graph theory. The analogy between an electric circuit and a directed graph with across and through variables is complete [30]. Kirchhoff's current and voltage laws are general postulates regarding incidence and circuit properties of directed graphs.

The fuse network circuit can be mapped onto a directed graph, where each link corresponds to a circuit element (a resistor or a voltage source) and the nodes simply correspond to circuit nodes. Each link is attributed a conductivity value G_j and has two variables: the current (through) i_j and the voltage (across) v_j. Kirchhoff's current law is simply stated as

$$\mathbf{Ai} = \mathbf{0} \tag{1}$$

where $\mathbf{A}$ is the reduced incidence matrix of the oriented graph representing the network.

A typical element of a resistive network [30] is shown in Fig. 2.

The subscript j indicates the jth element of the network and the subscript s indicates a generator or source. From Fig. 2, it follows

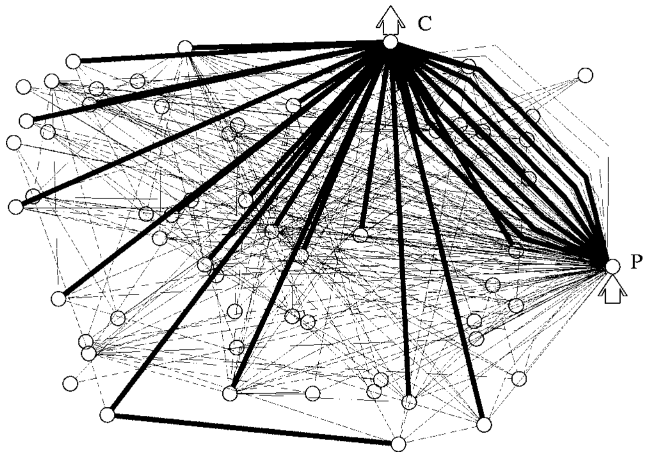

FIG. 3. Typical picture at final failure of network in loading case 1. Heavy lines are the burnt fuses. The central node is at the top marked by a large arrow departing from it. The periphery terminal is on the right, marked by a large arrow. The network is made small only for visualization purposes.

$$i_j = G_j v_j + i_{s,j} - G_j v_{s,j}, \quad j = 1,2, \ldots, e. \qquad (2)$$

e being the number of elements in the circuit or arcs in the graph. The set of equations (2) may be written in the vector form

$$\mathbf{i} = \mathbf{G}\mathbf{v} + \mathbf{i_s} - \mathbf{G}\mathbf{v_s}, \qquad (3)$$

where the conductivity matrix $\mathbf{G}$ is a diagonal matrix with each element G_{jj} corresponding to the conductivity of the jth circuit element.

The node analysis of the network, corresponding to Kirchhoff's current law Eq. (1), can now be expressed by

$$\mathbf{AGv} + \mathbf{Ai_s} - \mathbf{AGv_s} = \mathbf{0}. \qquad (4)$$

Now, if $\mathbf{v_n}$ denotes the nodes voltages relative to a chosen *datum* node, the vector $\mathbf{v}$ of voltages across each element may be written as

$$\mathbf{v} = \mathbf{A}^t \mathbf{v_n}. \qquad (5)$$

Using (5) in (4) and considering that our circuit is only fed by a voltage source ($\mathbf{i_s} = \mathbf{0}$), it comes

$$\mathbf{AGA}^t \mathbf{v_n} = \mathbf{AGv_s}. \qquad (6)$$

Defining the node admittance matrix $\mathbf{Y} = \mathbf{AGA}^t$, the network node analysis results in the expression

$$\mathbf{Y}\mathbf{v_n} = \mathbf{i_n} \qquad (7)$$

where $\mathbf{i_n} = \mathbf{AGv_s}$.

Since $\mathbf{Y}$ is invertible, $\mathbf{v_n}$ can be found by means of Eq. (7). Equation (5) will then give $\mathbf{v}$ and Eq. (3) will finally provide $\mathbf{i}$, the vector of currents through each element.

Once created the scale-free network, each one of its e links is made a fuse, all having the same conductivity $G_j = 1$ and the same tolerance $i_{c,j} = 1$. An external voltage $v_s = 1$ is then applied to this network, adding an extra element to the network. The vector $\mathbf{v_s}$, corresponding to the voltage sources, has only one nonzero element, that is its $(e+1)$th entry. In order to have $\mathbf{Y}$ invertible, the external voltage source has to be nonideal and its conductivity is also made unitary.

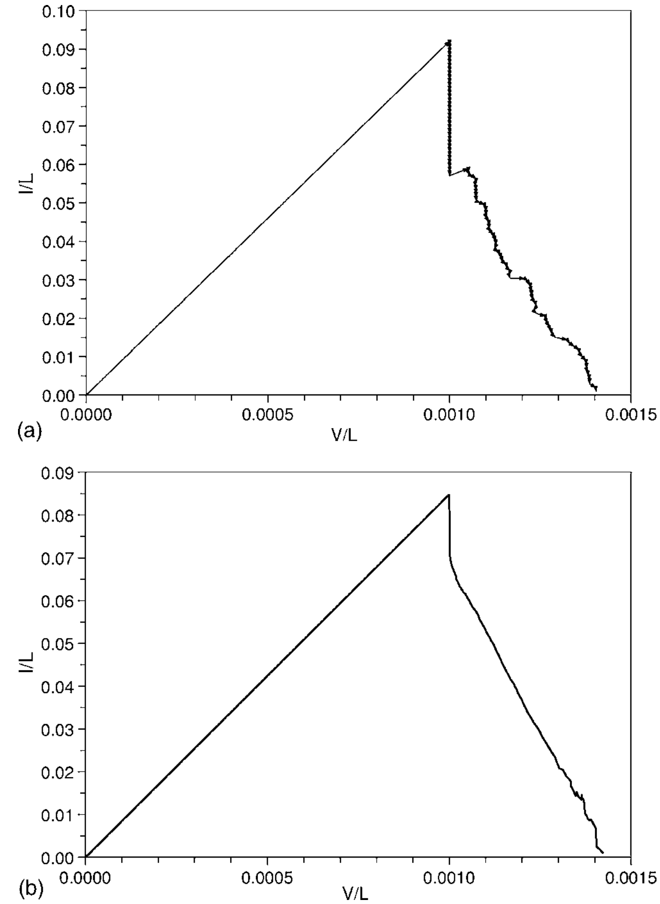

FIG. 4. *I-V* curve for load mode 1 for a network of 1000 nodes and 3000 fuses. (a) A single sample, with arrows showing the values of V and I for the burning sequence. (b) Average over 100 networks.

The test procedure for a single network begins with the inversion of $\mathbf{Y}$ to obtain $\mathbf{v_n}$, $\mathbf{v}$ and finally $\mathbf{i}$, by means of Eqs. (7), (5), and (3). The external voltage v_s is always set to 1, but the real voltage at the terminals of the voltage source is $v_{e+1} = v_s - G_{e+1} i_{e+1} = v_s - i_{e+1}$ (recalling that the index $e+1$ denotes the extra element added, that is, the voltage source).

The hottest fuse is the one with the maximum ratio $\lambda = i_j / i_{c,j}$, from now on, called λ_{max}. So, the external (real) voltage to burn the hottest fuse is $V = v_{e+1} / \lambda_{max}$, and the total current $I = i_{e+1} / \lambda_{max}$. The burning of a fuse means it is irreversibly removed from the network. The currents are recalculated and again the hottest fuse is removed for a new value of V and I, which will define a sequence (V_m, I_m), with m ranging from 1 to the last burning of a fuse, corresponding to the network breaking apart and no more current being conduced through it.

After the mth fuse connecting node r to node s is burnt and removed from the network, the new admittance matrix $\mathbf{Y}$ will be given by

$$\mathbf{Y}_{m+1} = \mathbf{Y}_m - G_{rs} \mathbf{w}\mathbf{w}^t$$

where $\mathbf{w}$ is a vector whose elements are given by

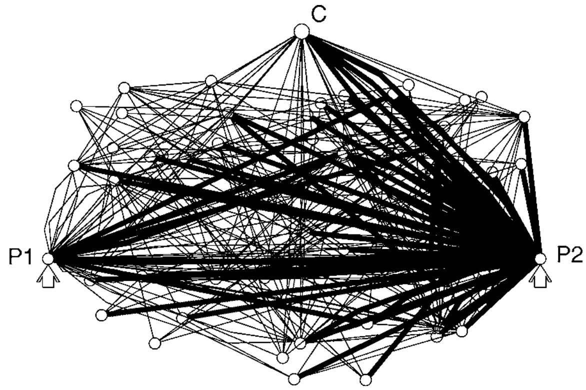

FIG. 5. Typical picture at final failure of network in loading case 2. Heavy lines are the burnt fuses. C indicates the central node; $P1$ and $P2$ are the two halves of the peripheral region. The network is made small for easier visualization.

$$w_r = 1$$

$$w_s = -1$$

$$w_j = 0, \quad \text{for } j \neq r \text{ and } j \neq s.$$

and G_{rs} is the conductance of the fuse that connects node r to node s. Significant computational advantages can be gained if the inverse of $\mathbf{Y_m}$ is simply updated by the well-known Shermon-Morrison-Woodbury formula. [31,32]

$$\mathbf{Y}_{m+1}^{-1} = \mathbf{Y}_m^{-1} + \left(f_{rs} \frac{\mathbf{u}\mathbf{u}^t}{(1 - G_{rs}\mathbf{w}^t\mathbf{u})} \right)$$

where

$$\mathbf{u} = \mathbf{Y}_m^{-1}\mathbf{w}.$$

The whole process is carried out using Scilab, the scientific software package, which has built-in graph tools.

IV. RESULTS AND DISCUSSION

A. Load mode 1

Load mode 1, as described earlier, refers to a central confluence of load, meaning that the links incident to this central load are the most likely to be overloaded. Figure 3 confirms that. It shows a small network at the end of simulation, when no more current is flowing because the system has broken down.

This is the typical result; all links incident to the central node failed. Sometimes an extra link would break, as in this case (the one at the very bottom).

The plot of current vs voltage for this load mode is shown in Fig. 4. L, in I/L and V/L, is the number of nodes, set to 1000 in all simulations in this section.

The profile seen in Fig. 4(b) resembles the stress-strain curve of a elastic material reinforced with fibers made of a tougher elastic material (like carbon fiber reinforced glass [2] and carbon fiber in carbonaceous matrix [1])—the fibers preventing the catastrophic one-crack failure.

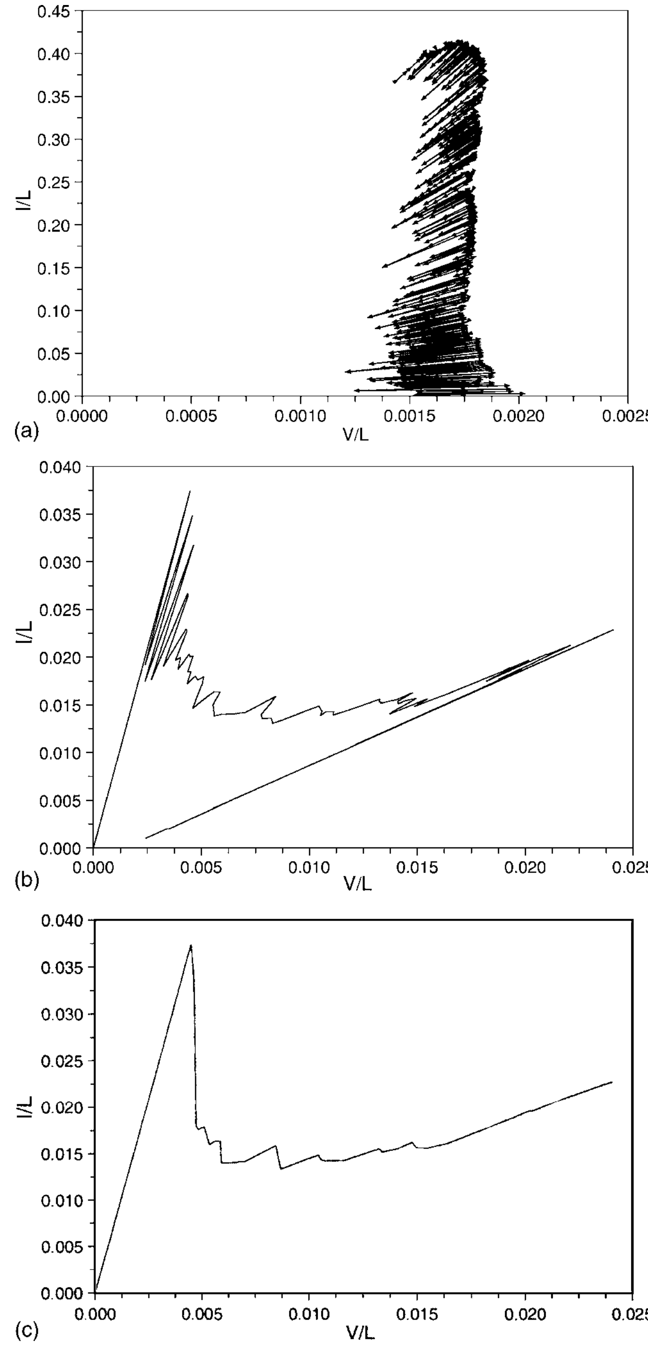

FIG. 6. I-V curve for load mode 2 for a network of 1000 nodes and 3000 fuses. (a) A single sample, with arrows showing the values of V and I for the burning sequence. (b) Average over 100 networks. (c) Voltage controlled test: same as (b), but allowing only increasing values of V.

B. Load mode 2

This mode, described earlier, would suggest escaping the total confluence toward the central node as seen in case 1. Nevertheless the rupture will be defined in one of the peripheral neighborhoods, as can be seen in Fig. 5.

Any imbalance between the two peripheral halves will trigger an avalanche in one of the "sides."

Figure 6 shows the behavior of the I vs V curve during the

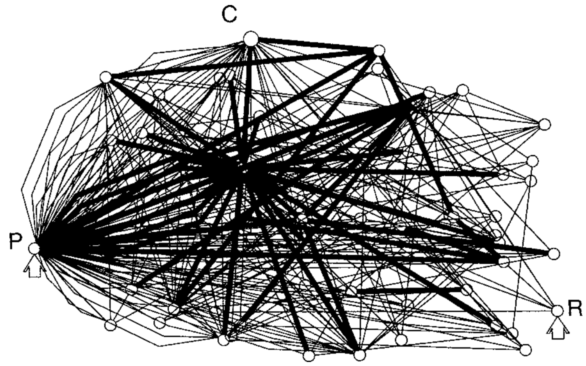

FIG. 7. Typical picture at final failure of network in loading case 3. Heavy lines are the burnt fuses. *C* indicates the central node (the most connected one). *P* denotes the periphery and *R* is the terminal connected to the randomly chosen nodes. The network is made small for easier visualization.

burning sequence for this case. In Fig. 6(a) it is possible to see significant oscillations observed for a single network. The arrows explicit the burning sequence. When averaged over 100 samples, the oscillations are significantly smoothed, as shown in Fig. 6(b).

If a voltage controlled test is considered, where *V* is made to increase monotonically and never decrease, the curve obtained is the one shown in Fig. 6(c). The mechanical correspondent would be the strain controlled test. It shows, in this case, a smooth transition not observed in either two other load cases. Mechanically it would represent fiber bridging, after matrix extensive microcracking, followed by fiber bundle failure [1,33].

C. Load mode 3

Another situation is described by case 3, also described earlier. Here the confluence toward the central node is relieved by setting a small fraction ($\sim 1\%$) of nodes to divide the flow toward the "central" terminal -as the one opposed to the periphery. The result is a spread of burned fuses as can be seen in Fig. 7.

The plot of current versus voltage in this case shows an interesting oscillation as can be seen in Fig. 8(a) and 8(b). For a single sample, it is interesting to note that after the first burn of a fuse, the three next fuses will burn in a decreasing sequence of overall tolerance (lower currents) of the network. Next, a significant raise in tolerance is seen, to be followed again by a decreasing sequence.

Along each lowering tolerance sequence, the overall conductivity of the network seems to remain nearly unchanged, since the values of *I* and *V*, in the sequence, lie on a straight line that intercepts the *V* axis next to the origin.

Averaging over 100 samples, *I* vs *V* curve still displays strong oscillations [Fig. 8(b)]. When the voltage controlled test is considered, with monotonically increasing *V*, the curve obtained is the one shown in Fig. 8(c).

V. CONCLUSIONS

The inherent inhomogeneity of scale-free networks has shown interesting consequences to the robustness of systems described by this kind of networks when their links are under load and subject to deterministic failure. Their characteristic distribution of incidence degrees has proved to be a major disorder element, with no need of further inhomogeneity distributions such as different load thresholds or different load response for the links.

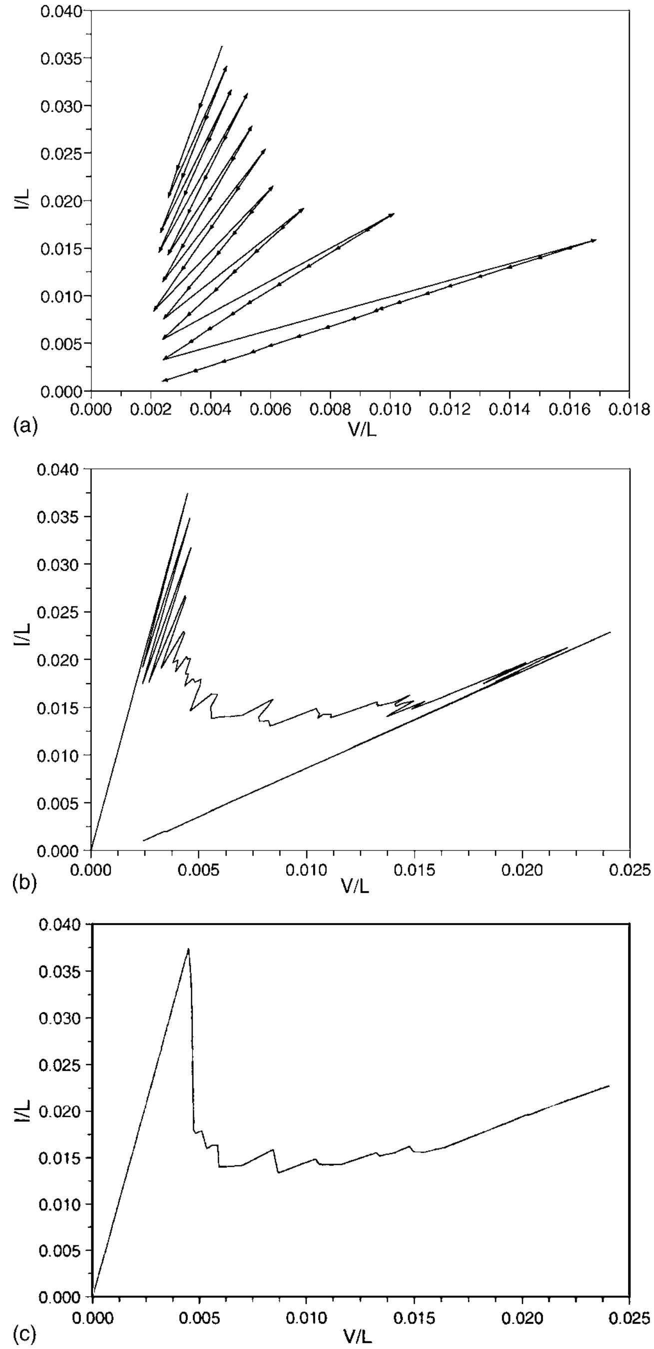

FIG. 8. *I*-*V* curve for load mode 3 for a network of 1000 nodes and 3000 fuses. (a) A single sample, with arrows showing the values of *V* and *I* for the burning sequence. (b) Average over 100 networks. (c) Voltage controlled test: same as (b), but allowing only increasing values of *V*.

Three different load modes have given place to three distinct breaking profiles. The distinctions were clear in both the load concentration geometry and overall load responses.

Larger scale tests with networks as large as 10^4 nodes and 3×10^4 links confirmed the load response profiles.

Although the fuse network may not be a direct mechanical model for the fracture problem it does seem to capture essential aspects of fracture in disordered media. Two of three modes shown here display load responses profiles with clear correspondence in fiber reinforced materials cases. That could suggest how internal stress fields in matrix and load share between fibers actually interact.

ACKNOWLEDGMENTS

C.F.S.P acknowledges R. F. Machado, and R. Rocha for first discussions on methods. This work was partially supported by the Brazilian agencies CAPES, FINEP, CNPq, and FAPEMIG. The large scale simulations were performed using the InfoCluster at the National Center for High Performance Computing—CENAPAD/MG-CO.

[1] K. K. Chawla, *Composite Materials—Science and Engineering* (Springer-Verlag, New York, 1987).
[2] H. J. Herrmann and S. Roux, *Statistical Models for the Fracture of Disordered Media* (Elsevier Science Publishers, New York, 1990).
[3] P. M. Duxbury, P. D. Beale, and P. L. Leath, Phys. Rev. Lett. **57**, 1052 (1986).
[4] B. Kahng, G. G. Batrouni, S. Redner, L. de Arcangelis, and H. J. Herrmann, Phys. Rev. B **37**, 7625 (1988).
[5] L. de Arcangelis and H. J. Herrmann, Phys. Rev. B **39**, 2678 (1989).
[6] G. G. Batrouni and A. Hansen, Phys. Rev. Lett. **80**, 325 (1998).
[7] S. Zapperi, P. Ray, H. E. Stanley, and A. Vespignani, Phys. Rev. E **59**, 5049 (1999).
[8] S. Zapperi, H. J. Herrmann, and S. Roux, Eur. Phys. J. B **17**, 131 (2000).
[9] R. Albert and A.-L. Barabási, Rev. Mod. Phys. **74**, 47 (2002).
[10] B. A. Huberman and L. A. Adamic, Nature (London) **401**, 131 (1999).
[11] R. Albert, H. Jeong, and A.-L. Barabási, Nature (London) **401**, 130 (1999).
[12] G. Caldarelli, R. Marchetti, and L. Pietronero, Europhys. Lett. **52**, 386 (2000).
[13] H. Jeong, S. Mason, A.-L. Barabási, and Z. N. Oltvai, Nature (London) **411**, 41 (2001).
[14] M. E. J. Newman, Phys. Rev. E **64**, 016132 (2001).
[15] D. J. Watts and S. H. Strogatz, Nature (London) **393**, 440 (1998).
[16] A.-L. Barabási and R. Albert, Science **286**, 509 (1999).
[17] A.-L. Barabási, R. Albert, and H. Jeong, Physica A **272**, 173 (1999).
[18] H. Stefancic and V. Zlatic, e-print cond-mat/0409648 (2004).
[19] R. Albert, H. Jeong, and A.-L. Barabsi, Nature (London) **406**, 378 (2000).
[20] R. Cohen, K. Erez, D. ben-Avraham, and S. Havlin, Phys. Rev. Lett. **85**, 4626 (2000).
[21] A. E. Motter, Phys. Rev. Lett. **93**, 098701 (2004).
[22] J.-L. Guillame, M. Latapy, and C. Magnien, *Comparison of Failures and Attacks on Random and Scale-Free Networks* (Springer-Verlag, Grenoble, 2005). Lect. Notes Comput. Sci. **3544**, 186–196 (2005)
[23] Y. Moreno, J. B. Gomez, and A. F. Pacheco, Europhys. Lett. **58**, 630 (2002).
[24] D. H. Kim, B. J. Kim, and H. Jeong, Phys. Rev. Lett. **94**, 025501 (2005).
[25] J. Chen, J. S. Thorp, and I. Dobson, Int. J. Electron. **27**, 318 (2005).
[26] B. A. Carreras, V. E. Lynch, I. Dobson, and D. E. Newman, Chaos **12**, 985994 (2002).
[27] I. Dobson, J. Chen, J. S. Thorp, B. A. Carreras, and D. E. Newman, in *Proceedings of the 35th Hawaii International Conference on System Sciences, Hawaii, 2002*, (IEEE Computer Soc., Big Island, (2002).
[28] A.-L. Barbási and E. Bonabeau, Sci. Am. **288**, 50 (2003).
[29] A.-L. Barabsi, *Linked: The New Science of Networks* (Perseus Publishing, Cambridge, 2002).
[30] D. E. Johnson and J. R. Johnson, *Graph Theory with Engineering Applications* (The Ronald Press Company, New York, 1972).
[31] G. H. Golub and C. F. van Loan, *Matrix Computations* 3rd ed. (The Johns Hopkins University Press, Baltimore, 1996).
[32] P. Kumar, V. V. Nukala, and S. Simunovic, J. Phys. A **36**, 11403 (2003).
[33] D. J. Green, *An Introduction to the Mechanical Properties of Ceramics* (Cambridge University Press, Cambridge 1998).